JOURNAL OF AIRCRAFT
Vol. 32, No. 6, November–December 1995

Nonlinear Analysis of Graphite/Epoxy Wing Boxes Under Pure Bending Including Lateral Pressure

Giulio Romeo* and Giacomo Frulla†
Politecnico di Torino, Turin 10129, Italy

Additional loads are created on wing-box panels when bending loads are applied to the box beam. Bending curvature, associated with longitudinal load, causes a distributed load perpendicular to both upper and lower wing-box panels resulting in a lateral pressure. The nonlinear analysis of anisotropic panels with initial imperfections has been developed for symmetric panels under combined biaxial compression, shear loads, and lateral pressure in order to obtain the out-of-plane panel deflection in the pre- and postbuckling range. The nonlinear differential equations are expressed in terms of the out-of-plane displacement and the Airy function. They are solved with the Galerkin method for various boundary conditions. Only by taking into account the nonlinear effects of the lateral pressure on the skin panels is it possible to obtain a good correlation between theoretical and experimental behavior. Experimental results on graphite/epoxy wing-box beams under pure bending showed remarkable deformations of the panels (particularly the compressed panel) in a direction normal to their centroidal surface, affecting both local strain values and the failure load value of the structures. Due to the effect of the lateral pressure, the blade-stiffened panel wing box showed a remarkable deformation also in the prebuckling field.

Nomenclature

$[A]$, $[D]$	= extensional and flexural stiffness matrices
a, b, h	= length, width, and thickness of panel
C_{pq}	= unknown coefficients for the out-of-plane function W
$(EI)_{na}$	= bending stiffness of wing-box beam respect to neutral axis
E_1, E_2	= lamina modulus in longitudinal and transverse directions
F	= nondimensional Airy function, $\psi/A_{22}h^2$
F_{hk}	= unknown coefficients for ψ
G_{12}	= lamina shear modulus
k	= curvature
M_b	= bending moment
M_x, M_y, M_{xy}	= moments per unit length
N_x, N_y, N_{xy}, N_z	= forces per unit length
q	= lateral pressure
T	= nondimensional maximum initial imperfection, w_0/h
t_e	= equivalent thickness of the stiffened panel
u, v, w	= displacement components
W	= nondimensional out-of-plane deflection, w/h
w_0	= initial imperfection
x, y, z	= Cartesian coordinates
Z_{na}	= vertical distance of panel centroid from neutral axis
ε_x, ε_y, ε_{xy}	= panel strain components
ε_x^0, ε_y^0, ε_{xy}^0	= midsurface strain components
η_ξ^*, η_η^*, $\eta_{\xi\eta}^*$	= nondimensional applied in-plane loads
λ	= plate AR, a/b
ν_{12}	= lamina Poisson's ratio
ξ, η, ζ	= nondimensional coordinate, x/a, y/b, z/h
ϕ	= slope of the neutral axis
ψ	= Airy function

Introduction

COMPOSITE aerospace structures are often designed so that they will not buckle below the limit load. However, many of the analytical and experimental results available in the literature[1–9] have shown a noticeable postbuckling behavior of the composite panels before failure occurs, depending on the width-to-thickness ratio.

These panels are usually considered as subjected to in-plane loads and separately from the main structure; this is an erroneous approach because additional effects are created on the skin panels, e.g., when all of the wing-box beams are subjected to a bending moment. Let us consider a wing box made up of two skin panels and two webs (Fig. 1); as a result of the applied bending moment, the beam is curved. The bending curvature, associated with longitudinal load, causes a distributed load perpendicular to both the upper and lower wing-box panels, resulting in a lateral pressure.[10] In some cases this pressure can play an important role in the deformation of the panels and of their elements (skin and stiffeners), as well as affecting their buckling behavior.

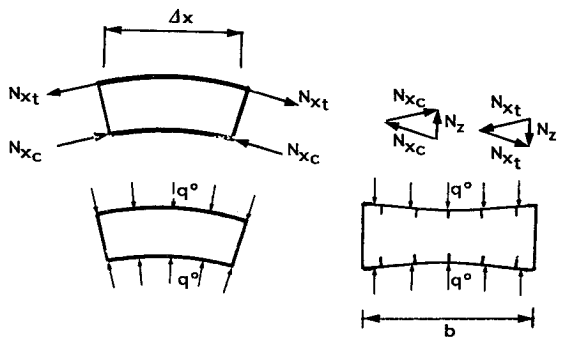

Fig. 1 Wing-box structure under pure bending.

Received March 21, 1994; revision received April 15, 1995; accepted for publication May 29, 1995.

*Associate Professor of Design of Aerospace Structures, Corso Duca degli Abruzzi 24.
†M.Sc., Aeronautical Engineering.

The effects of lateral pressure on the design of stiffened compression panels have been evaluated in the past[11-13] by superimposing the stress resulting from the moment produced by the lateral pressure, on the stress due to the applied longitudinal load. This procedure is applicable only when the applied load is much lower than the buckling load.

The deflection of the orthotropic rectangular plate under combined lateral and in-plane loads has been investigated by Chia.[14] The nonlinear terms have been included in this analysis and some theoretical results are reported for a simply supported plate. However, experimental results have not been obtained.

Deformations of wing-box compression panels were analytically investigated in the past[15] by using the differential equation of an orthotropic plate in which lateral pressure and initial imperfections are introduced into the analysis through a Fourier series. Only the linear terms were included in the strain-displacement relations; this means that the out-of-plane deflection tends to infinity as the applied load approaches the buckling load. However, experimental results on several aluminium–alloy wing-box beams in bending[16] showed remarkable deformations of panels in a direction normal to their barycentric surface, thereby affecting both local stresses and final failure load. The theoretical analysis of Ref. 15 was applied to two graphite/epoxy wing boxes under pure bending[17]; the same limitations as those reported previously have invalidated the comparison between the analytical and experimental results.

A nonlinear analysis is presented in this article to investigate the pre- and postbuckling behavior of simply supported and fully clamped anisotropic plates under combined biaxial compression, shear load, and lateral pressure. Since panels are often not perfectly manufactured, initial imperfections are also included in the analysis. Such imperfections, in fact, considerably influence the out-of-plane displacement behavior of the panel and cannot be ignored.

Theoretical Analysis

The classical laminate theory has to be modified for the large deflection and postbuckling analysis of anisotropic plates under combined biaxial compression, shear loads, and lateral pressure. The strain-displacement relations become nonlinear when the components due to the out-of-plane deflection are taken into account. Plates with the initial imperfections w_0 have been studied on the basis of the Marguerre approximate nonlinear theory.[14] The resultant strain-displacement relations are

$$\begin{aligned} \varepsilon_x &= u_{,x} + \tfrac{1}{2}w_{,x}^2 + w_{0,x}w_{,x} - zw_{,xx} \\ \varepsilon_y &= v_{,y} + \tfrac{1}{2}w_{,y}^2 + w_{0,y}w_{,y} - zw_{,yy} \\ \varepsilon_{xy} &= u_{,y} + v_{,x} + w_{,x}w_{,y} + w_{0,y}w_{,x} + w_{0,x}w_{,y} - 2zw_{,xy} \end{aligned} \tag{1}$$

An index separated by a comma represents a derivative. By introducing the Airy function $\psi(x, y)$ as

$$N_x = \psi_{,yy}, \qquad N_y = \psi_{,xx}, \qquad N_{xy} = -\psi_{,xy} \tag{2}$$

and by using the principle of the stationary value of the total potential energy, the third equilibrium equation is manipulated into[6]

$$\begin{aligned} &M_{x,xx} + M_{y,yy} + 2M_{xy,xy} + \psi_{,yy}w_{,xx} + \psi_{,xx}w_{,yy} - 2\psi_{,xy}w_{,xy} \\ &\quad + \psi_{,yy}w_{0,xx} + \psi_{,xx}w_{0,yy} - 2\psi_{,xy}w_{0,xy} + q = 0 \end{aligned} \tag{3}$$

The compatibility equation is introduced in conjunction with Eq. (3) for panels with initial imperfections as

$$\begin{aligned} &\varepsilon^0_{x,yy} + \varepsilon^0_{y,xx} - \varepsilon^0_{xy,xy} = w^2_{,xy} - w_{,xx}w_{,yy} \\ &\quad + 2w_{0,xy}w_{,xy} - w_{0,yy}w_{,xx} - w_{0,xx}w_{,yy} \end{aligned} \tag{4}$$

By substituting the stress–strain relations for symmetric panels, in terms of the ψ function and the out-of-plane displacement, in Eqs. (3) and (4), and normalizing as

$$[\bar{A}^*] = A_{22}[A^{-1}] \quad [\bar{D}^*] = \frac{1}{h^2A_{22}}[D] \quad \bar{q} = qa^4/E_2h^4 \tag{5}$$

the following governing system is obtained:

$$\begin{aligned} &\bar{D}^*_{11}W_{,\xi\xi\xi\xi} + 4\bar{D}^*_{16}\lambda W_{,\xi\xi\xi\eta} + 2(\bar{D}^*_{12} + 2\bar{D}^*_{66})\lambda^2 W_{,\xi\xi\eta\eta} \\ &\quad + 4\bar{D}^*_{26}\lambda^3 W_{,\xi\eta\eta\eta} + \bar{D}^*_{22}\lambda^4 W_{,\eta\eta\eta\eta} - \lambda^2(F_{,\eta\eta}W_{,\xi\xi} \\ &\quad + F_{,\xi\xi}W_{,\eta\eta} - 2F_{,\xi\eta}W_{,\xi\eta} + F_{,\eta\eta}W_{0,\xi\xi} + F_{,\xi\xi}W_{0,\eta\eta} \\ &\quad - 2F_{,\xi\eta}W_{0,\xi\eta}) - \bar{q} = 0 \end{aligned} \tag{6}$$

$$\begin{aligned} &\bar{A}^*_{11}\lambda^4 F_{,\eta\eta\eta\eta} - 2\bar{A}^*_{16}\lambda^3 F_{,\xi\eta\eta\eta} + (2\bar{A}^*_{12} + \bar{A}^*_{66})\lambda^2 F_{,\xi\xi\eta\eta} \\ &\quad - 2\bar{A}^*_{26}\lambda F_{,\xi\xi\xi\eta} + \bar{A}^*_{22}F_{,\xi\xi\xi\xi} = \lambda^2(W^2_{,\xi\eta} - W_{,\xi\xi}W_{,\eta\eta} \\ &\quad + 2W_{0,\xi\eta}W_{,\xi\eta} - W_{0,\eta\eta}W_{,\xi\xi} - W_{0,\xi\xi}W_{,\eta\eta}) \end{aligned} \tag{7}$$

The usual four types of boundary conditions along the edges of the panel are studied[6]: 1) ends simply supported, sides simply supported (BC-1); 2) ends clamped, sides simply supported (BC-2); 3) ends clamped, sides clamped (BC-3); and 4) ends simply supported, sides clamped (BC-4).

Several conditions have to be satisfied for each boundary. For example, for (BC-4)

$$\begin{aligned} &\xi = 0, 1: \quad F_{,\eta\eta} = \eta^*_\xi \quad F_{,\xi\eta} = -\lambda\eta^*_{\xi\eta} \quad W = 0 \quad M_\xi = 0 \\ &\eta = 0, 1: \quad F_{,\xi\xi} = \lambda^2\eta^*_\eta \quad F_{,\xi\eta} = -\lambda\eta^*_{\xi\eta} \quad W = 0 \quad W_{,\eta} = 0 \end{aligned} \tag{8}$$

where the nondimensional applied in-plane loads η^*_ξ, η^*_η, $\eta^*_{\xi\eta}$ are given as

$$\eta^*_\xi = \frac{N_xb^2}{h^2A_{22}} \qquad \eta^*_\eta = \frac{N_yb^2}{h^2A_{22}} \qquad \eta^*_{\xi\eta} = \frac{N_{xy}b^2}{h^2A_{22}} \tag{9}$$

To satisfy the boundary conditions the assumed functions are chosen in the following form:

$$F = \eta^*_\xi\eta^2/2 + \eta^*_\eta\lambda^2\xi^2/2 - \lambda\eta^*_{\xi\eta}\xi\eta + \sum_{h=1}^{m}\sum_{k=1}^{n} F_{hk}X_h(\xi)Y_k(\eta) \tag{10}$$

$$W = \sum_{p=1}^{i}\sum_{q=1}^{j} C_{pq}\omega(\xi, \eta) \tag{11}$$

$$W_0(\xi, \eta) = T\sin(\pi\xi)\sin(\pi\eta) \tag{12}$$

where X and Y are the characteristic clamped–clamped beam functions.[6] While the Airy function remains the same, the function $\omega(\xi, \eta)$ is chosen according to the boundary conditions to be

1) BC-1 $\omega(\xi, \eta) = \sin(h\pi\xi)\sin(k\pi\eta)$
2) BC-2 $\omega(\xi, \eta) = X_h(\xi)\sin(k\pi\eta)$
3) BC-3 $\omega(\xi, \eta) = X_h(\xi)Y_k(\eta)$
4) BC-4 $\omega(\xi, \eta) = \sin(h\pi\xi)Y_k(\eta)$

The nondimensionalized transverse load $\bar{q}$ has been expanded in double trigonometric series as

$$\bar{q} = \sum_m\sum_n q_{mn}\sin(m\pi\xi)\sin(n\pi\eta) \tag{13}$$

If the load $\bar{q}$ is uniform, then

$$q_{mn} = \begin{cases} 16\bar{q}^0/\pi^2mn & \text{for odd} \quad m, n \\ 0 & \text{for even} \quad m, n \end{cases} \tag{14}$$

Solution Method

A set of nonlinear algebraic equations (the governing system) in terms of F_{hk} and C_{pq} and in terms of calculated Galerkin coefficients has been obtained by using the Galerkin procedure in Eqs. (6) and (7). The resultant nonlinear algebraic equations in the contracted form are

$$\sum_{mn} C_{mn} D^{ij}_{mn} = \sum_{pq} C_{pq} K^{ij}_{pq} + \sum_{pqrs} C_{pq} F_{rs} G^{ij}_{pqrs} + T\left(K0^{ij} + \sum_{rs} F_{rs} G0^{ij}_{rs}\right) + Q^{ij} \quad (15)$$

$$\sum_{mn} F_{mn} A^{ij}_{mn} = \sum_{pqrs} C_{pq} C_{rs} B^{ij}_{pqrs} + T \sum_{pq} C_{pq} B0^{ij}_{pq} \quad (16)$$

The terms A^{ij}_{mn}, B^{ij}_{pqrs}, D^{ij}_{mn}, G^{ij}_{pqrs}, and K^{ij}_{pq} concern the situation without an initial imperfection T. The terms $B0^{ij}_{pq}$, $G0^{ij}_{rs}$, and $K0^{ij}$ concern the presence of T, and Q^{ij} relates the presence of external transverse load. These all vary according to various geometric parameters, materials, boundary conditions, and Galerkin integrals. The applied loads are contained in the terms K^{ij}_{pq}, $K0^{ij}$, and Q^{ij}. Although a good convergence of the Galerkin solution has been obtained with 25 terms, it is preferable to use 36 terms.

The Pobuck computer program[6] has been developed to solve the set of nonlinear equations (15) and (16), using an iterative procedure in order to find the postbuckling path at a certain load level. After possible values have been assigned to the unknowns C_{pq}, the first step consists of extracting F_{hk} from Eq. (16) and substituting it into Eq. (15). The next step is to solve this final nonlinear system as a function of the C_{pq} unknowns and thereby work out the C_{pq}. The scientific library software available from ABACI is then employed to solve the final nonlinear system, using as a base the modified Powell hybrid method for finding the zero of a system of nonlinear functions.[18,19] The user provides a subroutine that calculates the functions and the ABACI code calculates the Jacobian by a forward-difference approximation. The iteration is developed until convergence with C_{pq} is reached, within 0.5%. The new minimum total potential energy configuration (also with different numbers of half-waves) is obtained, starting with the last solution of C_{pq} for subsequent load levels. If convergence has not been reached in this way, different initial C_{pq} values can be assigned. The ABACI software used for solving the nonlinear system quickly converges to a solution without noticeable problems.

The Pobuck software operates on an IBM PS2 or higher, requiring about 5 min of CPU time with 36 terms, using NDP Fortran.

Lateral Pressure

As the result of the bending curvature, the longitudinal load applied in the upper and lower wing-box panels are not aligned with respect to each other (Fig. 1); a vector addition therefore results in a lateral load per unit width $N_z = N_x\phi$. On the assumption that the engineer's theory of bending (ETB) holds, the variation of the lateral load between an infinitesimal length x is given by

$$N_{z,x} = N_x\phi_{,x} = N_x w_{,xx} = N_x k_{\text{ETB}} \quad (17)$$

since

$$N_x = M_b Z_{\text{na}} t_e / I_{\text{na}} \qquad k_{\text{ETB}} = M_b/(EI)_{\text{na}} \quad (18)$$

The lateral pressure q^0 applied to each of the wing-box anisotropic panels is finally calculated as

$$q^0 = M_b^2 (A_{11} - A_{12}^2/A_{22}) Z_{\text{na}}/(EI)^2_{\text{na}} \quad (19)$$

Out-of-Plane Deflection and Curvature

Within the ETB hypothesis, deflection and curvature of a box beam subjected to pure bending are given by

$$w_{\text{ETB}} = M_b(ax - x^2)/2(EI)_{\text{na}} \qquad k_{\text{ETB}} = M_b/(EI)_{\text{na}} \quad (20)$$

If the local deformations due to the lateral loads are not considered significant, these two parameters would be constant along the width of the wing box. For example, a determined value of the length gives a wing-box deflection $w_{\text{N.L.}}$ of the same value as in the lateral section as well as in the middle section. The whole out-of-plane panel deflection is finally obtained by superimposing the nonlinear deflection $w_{\text{N.L.}}$ of the panel subjected to combined uniaxial compression and lateral load [Eqs. (15) and (16)], on the wing-box beam deflection obtained by the ETB [Eq. (20)]. Along the sides, of course, the nonlinear contribution is zero since the panel is supported. The same procedure is followed for the panel curvature:

$$w = w_{\text{N.L.}} + w_{\text{ETB}} \qquad k = k_{\text{N.L.}} + k_{\text{ETB}} \quad (21)$$

Experimental Tests

An original testing machine was built[15,16] in order to apply pure bending loads to wing-box beams (Fig. 2); the apparatus consists of a frame (A), two spar clamps (B), hinged through bolts to four swinging linkrods (C), and two hydraulic jacks (D). The specimen (E) is bolted with suitable fittings to the clamps; a hydraulic jack is hinged to the other side of each clamp so that the bending moment can be applied step-by-step.

Several bending tests were carried out on wing-box beams.[13,17] Graphite/epoxy prepreg material was used for manufacturing the specimens and cured by means of an autoclave cure cycle. One specimen had blade-stiffened cross-sectional panels with lamina stacking sequence and dimensions as shown in Fig. 3. A moderate difference was measured between the thicknesses of the compression and tension panel elements. Since the

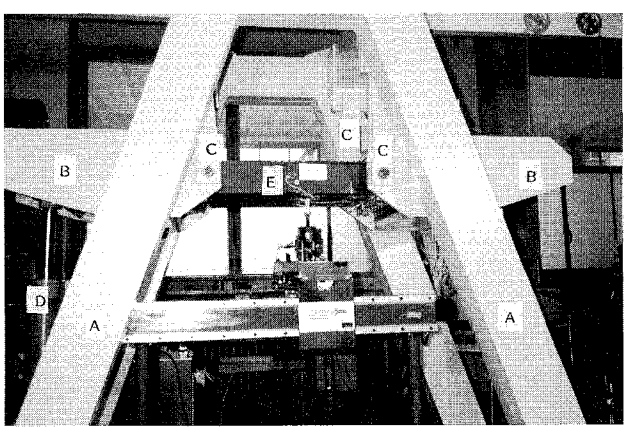

Fig. 2 Overall view of the bending machine.

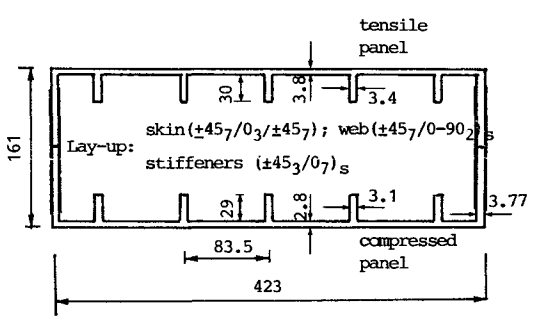

Fig. 3 Configuration and geometrical data of the wing box tested under bending.

Table 1 Buckling analytical results for the wing-box stiffened panel under uniaxial compression

Buckling mode	Buckling load, N/mm	Applied load, N/mm	
Overall	−488	−488	−563
Skin	−716	−251	−289
Stiffener	−852	−688	−794
Torsional	−1212	−488	−563

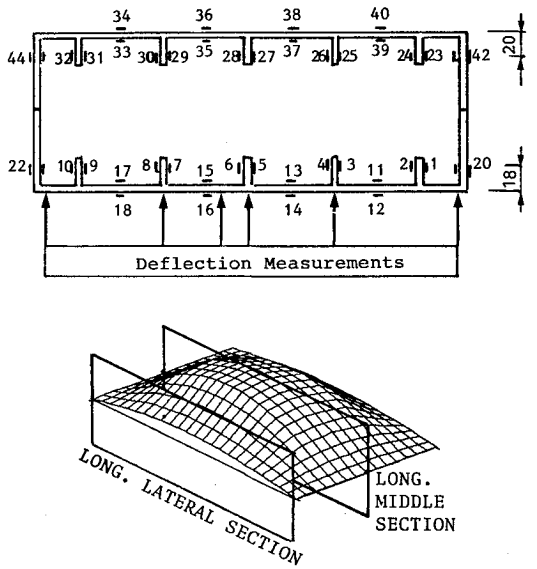

Fig. 4 Strain gauges and deflection measurement locations.

same layup was used for both panels, this difference seems due to improper vacuum bagging and consequent pressure application during the two cure cycles. The wing-box length (excluding the fittings) was 0.688 m.

Deflection data at different load levels were taken by using a dial deflectometer that ran on a guide independent of the box structure for a length of approximately 0.43 m and was connected to an $x - y$ recorder. Longitudinal strains were measured by several strain gauges placed back-to-back at panel half-lengths (Fig. 4).

The lamina material properties were experimentally determined to be

tape: $E_1 = 131.08$ GPa $E_2 = 13.01$ GPa $G_{12} = 6.41$ GPa $\nu_{12} = 0.38$.
fabric: $E_1 = 63.76$ GPa $E_2 = 63.76$ GPa $G_{12} = 6.41$ GPa $\nu_{12} = 0.08$.

The smeared extensional and bending stiffnesses[12,20,21] of the stiffened panel with respect to the centroidal axis were

$A_{11} = 254{,}983$, $A_{12} = 70{,}680$, $A_{22} = 104{,}934$, $A_{66} = 74{,}296$ (N/mm)
$D_{11} = 19{,}163{,}138$, $D_{12} = 71{,}006$, $D_{22} = 75{,}478$, $D_{66} = 74{,}448$ (Nmm)

The theoretical overall buckling load of the stiffened panel subjected to uniaxial compression was determined via the computer code Pobuck introducing the smeared stiffnesses[12,20,21] in the plate governing system [Eqs. (15) and (16)]. The local skin buckling is determined in the same way by introducing the skin stiffnesses in place of the smeared stiffnesses. Furthermore, the local buckling of the stiffeners, as well as the torsional buckling, were determined.[13,20] The boundary conditions considered along the edges of the panel were with the sides clamped and the ends simply supported. A summary of the results obtained is reported in Table 1. The analytical buckling mode and buckling load are shown; for two values of the load applied in the compression panel during the test (−488 and −563 N/mm), and the load distribution between skin and stiffeners is also noted. At the highest load applied during the test, the stiffener applied load is very close to the stiffener buckling load.

Experimental Results

A summary of the analytical and experimental results obtained is given in Table 2.

The deflection curves were measured on the compression panel along the wing-box length at several longitudinal sections (Fig. 4). Two were near the side webs (lateral sections), one was along the longitudinal middle section in correspondence to a stiffener, one was along the skin between two

Table 2 Analytical results for the wing-box stiffened panel under pure bending

M_b, kNm	N_x, N/mm	q^0, MPa	$w_{N.L.}$, mm	$k_{xN.L.} \times 10^6$ 1/mm
7.18	−93.7	0.00062	0.181	3.7
14.36	−187.5	0.0025	0.795	16.4
17.95	−234.3	0.0039	1.41	29.0
21.54	−281.2	0.0056	2.38	49.0
25.13	−328.1	0.0076	3.86	79.4
28.72	−375.0	0.0099	5.91	121.0
32.31	−421.9	0.0126	8.34	169.4
35.9	−468.8	0.0155	10.81	216.8
39.49	−515.5	0.0188	13.19	261.2

$(EI)_{na} = 1.0816\text{E}12$, Nmm²

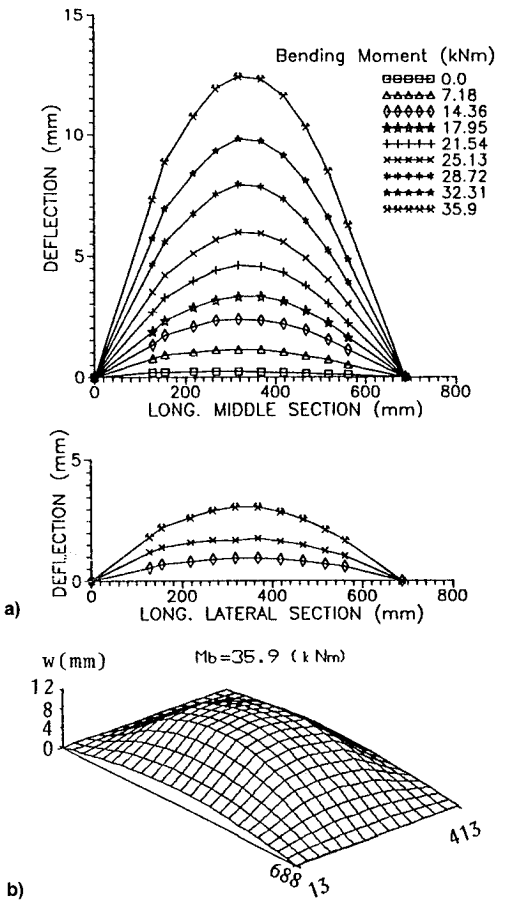

Fig. 5 Experimental out-of-plane deflection of the compressed wing-box stiffened panel: a) longitudinal middle section (above) and lateral section (below) and b) axonometric view at a bending moment of 35.9 kNm.

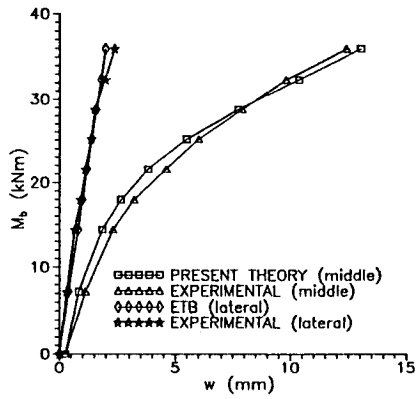

Fig. 6 Comparison between the experimental and the analytical out-of-plane deflection.

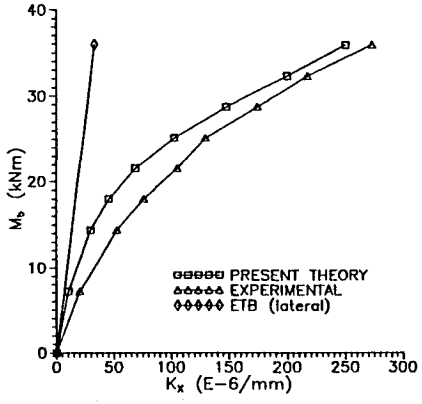

Fig. 7 Comparison between the experimental and the analytical panel curvature.

stiffeners (not exactly at the half-pitch because of the strain gauge location), and two were along the stiffeners. An initial imperfection was recorded on the compression panels. The highest values measured were 0.25 mm on the middle width and 0.1 mm at the sides.

The deflection curves measured along the longitudinal middle and lateral sections are drawn in Fig. 5a for different values of the applied bending moment. A remarkable difference between the two longitudinal sections can be seen clearly, as well as in the axonometric view (Fig. 5b). Within the ETB hypothesis, beams should have the same deflection along the entire width of the same transverse section (webs, middle, etc.). It is only by taking into account the effect of the lateral pressure produced by the beam curvature (as reported in the present analysis) that the discrepancy can be justified. A comparison between the experimental and the whole analytical out-of-plane deflection is shown in Fig. 6. The maximum deflection of the compressed stiffened panel (measured at half length) is plotted as a function of the applied bending moment. Both the middle deflections and the lateral deflections are reported. The linear behavior traced here was determined by Eq. (20) and it is only valid for the lateral section. The linear behavior clearly varies considerably from the experimental results measured in the middle section. Overall, a good correlation was obtained between the results determined by the present nonlinear analysis and experiment. The same behavior is shown for the whole panel curvature along the x axis (Fig. 7). The theoretical curvature was obtained by using the second derivative of the analytical panel deflection along the panel length; while the experimental curvature was analytically obtained from the experimental deflection along the panel length. The analytical and the experimental results differed only slightly here.

Figure 8 shows the experimental strains as a function of the applied bending moment, measured by back-to-back gauges

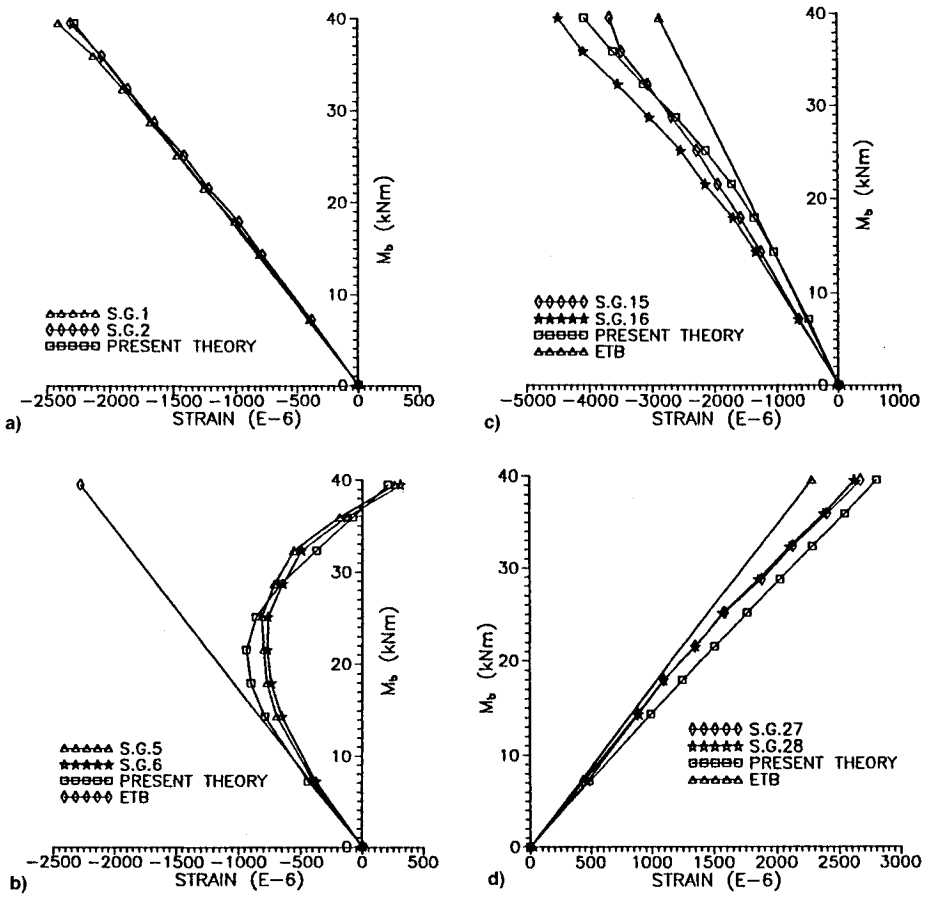

Fig. 8 Comparison between the experimental and the analytical longitudinal strains.

placed both on the skin and on the stiffeners as outlined in Fig. 4. An almost linear behavior (Fig. 8a) was recorded on the compressed stiffener placed near the web (gauges no. 1–2). Here, the panel curvature exerts little influence on the classical bending strain. A totally different behavior (Fig. 8b) is observed in the compressed stiffener placed in the middle section (gauges no. 5–6). It clearly varies from the classical ETB and a strain reversal occurred starting at a bending moment of 23.33 kNm. Since both back-to-back strain gauges behaved in the same way, local stiffener buckling is excluded. As an effect of the lateral pressure, the stiffener was subjected to a local bending moment that drastically alters the hypothesis of a uniform compression longitudinal loading of the panel. In practice, a tensile value was obtained at the maximum moment data recorded. All things considered, a good correlation was obtained between the results determined by the present nonlinear analysis and the experiment. Strains were analytically determined by superimposing the strain resulting from the lateral pressure curvature on the classical bending strain of the centroid, and the local deflection was taken into account on the vertical distance of each element with respect to the neutral axis

$$\varepsilon_{xi} = \varepsilon^0_{xi} \pm z_{ci}k_x = M_b Z_{na}/(EI)_{na} \pm z_{ci}k_x \qquad (22)$$

The same behavior was recorded for gauges no. 3–4 and no. 7–8. Contrary to the behavior of the compressed stiffener above the centroid, the strain of the compressed skin panel (gauges no. 15–16) is increased by the lateral pressure curvature (Fig. 8c). A strain reversal typical of local skin buckling seems to begin at the maximum moment data recorded. An almost linear behavior was observed in the tensile panel, both for the stiffeners (gauges no. 27–28) (Fig. 8d) and for the skin. Lateral pressure also affects the strain distribution, but less so.

The plot of compression membrane longitudinal strains across the panel width at different moment levels is shown in Fig. 9a for the skin and 9b for the stiffeners and webs. We can clearly see the nonlinear effects of the lateral pressure, especially on the stiffeners. At the highest load reached in the test, only two of the five stiffeners were still subjected to compression while the other three were loaded in tension.

The wing box failed at a bending moment of 43.1 kNm (which corresponds to a longitudinal load of 563 N/mm) by delamination of the compression stiffener at about 90 mm from one end. Although applied strains are not well documented, since there were no strain gauges placed in that area, it seems possible that failure occurred as a result of the local buckling of the stiffeners. Several experimental tests[13] showed that stiffened panels under uniaxial compression failed catastrophically as the applied load approched the buckling load. However in our tests, as reported in Table 1, the applied longitudinal load was greater than the predicted overall buckling load. This event could be a consequence of the nonuniform compression longitudinal loading of the stiffened panel.

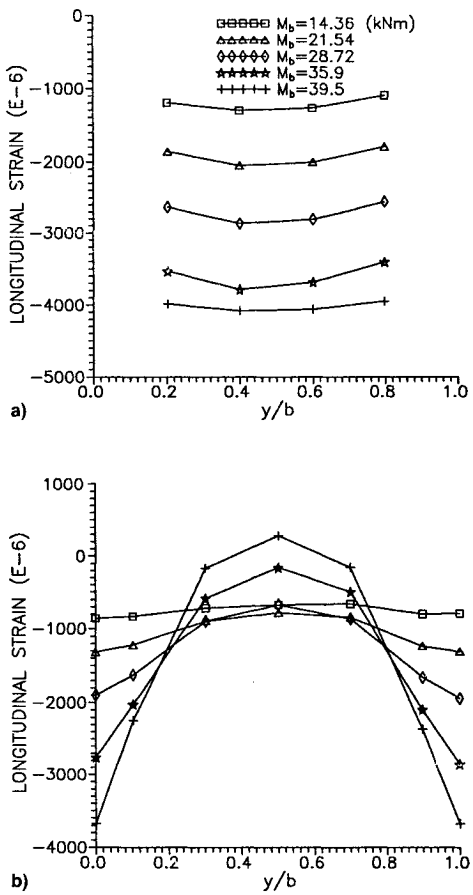

Fig. 9 Compression membrane longitudinal strains across the panel width at different bending moments: a) skin and b) stiffeners and webs.

Conclusions

A good correlation between theoretical analysis and experimental results was obtained for wing boxes under pure bending by considering the nonlinear effects of the lateral pressure on the deflections of stiffened panels. These tests clearly demonstrate that lateral pressure can drastically change the buckling of stiffened panels and the strain distribution on each element.

Experimental results permit the following conclusions:

1) The Pobuck computer program is well structured and gives results consistent with the experiment.

2) Extended testing activity is necessary to investigate other boundary conditions and to verify the behavior for higher loads.

3) Results were obtained for a flat panel with initial imperfections, however, a light curvature is induced along the panel length due to the bending moment. Therefore, the governing system has to be modified in order to include this effect.

Further efforts should be directed towards the examination of these problems with a view to improve the correlation between theoretical and experimental data.

References

[1]Stein, M., "Postbuckling of Long Orthotropic Plates Under Combined Loading," *AIAA Journal*, Vol. 23, No. 8, 1985, pp. 1267–1272.

[2]Starnes, J. H., Dickson, J. N., and Rouse, M., "Postbuckling Behaviour of Graphite-Epoxy Panels," *Proceedings of ACEE Composite Structures Technology*, 1984, pp. 137–159 (NASA CP-2321).

[3]Engelstad, S. P., Reddy, J. N., and Knight, N. F., Jr., "Postbuckling Response and Failure Prediction of Graphite-Epoxy Plates Loaded in Compression," *AIAA Journal*, Vol. 30, No. 8, 1992, pp. 2106–2113.

[4]Zhang, Y., and Matthews, F. L., "Postbuckling Behaviour of Anisotropic Laminated Plates Under Pure Shear and Shear Combined with Compressive Loading," *AIAA Journal*, Vol. 22, No. 2, 1984, pp. 281–286.

[5]Sheinman, I., Frostig, Y., and Segal, A., "Nonlinear Analysis of Stiffened Laminated Panels with Various Boundary Conditions," *Journal of Composite Materials*, Vol. 25, No. 9, 1991, pp. 634–649.

[6]Romeo, G., and Frulla, G., "Nonlinear Analysis of Anisotropic Plates with Initial Imperfections and Various Boundary Conditions Subjected to Combined Biaxial Compression and Shear Loads," *International Journal of Solids and Structures*, Vol. 31, No. 6, 1994, pp. 763–783.

[7]Leissa, A. W., "Buckling of Laminated Composite Plates and Shell Panels," Air Force Wright Aeronautical Labs., AFWAL-TR-

85-3069, Wright–Patterson AFB, OH, 1985.

[8]Hui, D., "Effect of Geometric Imperfections on Large Amplitude Vibrations of Rectangular Plate with Hysteresis Damping," *Journal of Applied Mechanics*, Vol. 51, No. 4, 1983, pp. 750–756.

[9]Kapania, R. K., and Yang, T. Y., "Buckling, Postbuckling, and Nonlinear Vibrations of Imperfect Plates," *AIAA Journal*, Vol. 25, No. 10, 1987, pp. 1338–1346.

[10]Kuhn, P., *Stresses in Aircraft and Shell Structures*, 1st ed., McGraw–Hill, New York, 1956.

[11]Giles, G. L., and Anderson, M. S., "Effects of Eccentricities and Lateral Pressure on the Design of Stiffened Compression Panels," NASA TN D-6784, June 1972.

[12]Stroud, W. J., and Anderson, M. S., "PASCO: Stuctural Panel Analysis and Sizing Code, Capability and Analytical Foundations," NASA TM-80181, Nov. 1981.

[13]Romeo, G., "Experimental Investigation on Advanced Composite Stiffened Structures Under Uniaxial Compression and Bending," *AIAA Journal*, Vol. 24, No. 11, 1986, pp. 1823–1830.

[14]Chia, C. Y., *Nonlinear Analysis of Plates*, McGraw–Hill, New York, 1980.

[15]Antona, E., and Pelagalli, P., "Analisi Strutturale dei Cassoni Alari Bilongheroni Soggetti a Flessione in Campo Eiastico" ("Structural Analysis of Two-Spar Wing Boxes with Elastic Behaviour Under Bending"), Dept. of Aerospace Eng., Rept. 49, Politecnico di Torino, Italy, Dec. 1968 (in Italian).

[16]Gabrielli, G., and Antona, E., "An Experimental Investigation on Wing Box Beams in Bending," International Council of the Aeronautical Sciences, Paper 70-33, Rome, Italy, Sept. 1970.

[17]Antona, E., and Romeo, G., "Analytical and Experimental Investigation on Advanced Composite Wing Box Structures in Bending Including Effects of Initial Imperfections and Crushing Pressure," *Proceedings of the 15th ICAS Congress* (London, GB), Vol. I, AIAA, New York, 1986, pp. 255–261.

[18]Powell, M. J. D., "A Hybrid Method for Nonlinear Equations," *Numerical Methods for Nonlinear Algebraic Equations*, edited by P. Rabinowitz, Gordon and Breach, New York, 1970.

[19]Abaci, C., *The Scientific Desk—User Guide*, ABACI, Raleigh, NC, 1987.

[20]Romeo, G., and Baracco, A., "Minimum-Mass Optimization of Composite Stiffened, Unstiffened and Sandwich Curved Panels Subjected to Combined Longitudinal and Transverse Compression and Shear Loading," *Proceedings of the 7th International Conference on Composite Materials (ICCM)* (Canton, PRC), Vol. 3, Pergamon, Oxford, England, UK, 1989, pp. 364–370.

[21]Stroud, W. J., and Agranoff, N., "Minimum-Mass Design of Filamentary Composite Panels Under Combined Loads: Design Procedure Based on Simplified Buckling Equations," NASA TN D-8257, Oct. 1976.